

Biallelic *Dicer1* loss mediated by *aP2-Cre* drives angiosarcomagenesis

Jason A. Hanna, Catherine J. Drummond, Matthew R. Garcia, Jonathan C. Go, David Finkelstein, Jerold E. Rehg, and Mark E. Hatley

Supplementary Information Inventory

Supplementary Tables

Table S1. Enrichr analysis of miRNA targets in angiosarcoma.

Table S2. Antibodies used for immunohistochemistry.

Table S3. Real-time SYBR primers and PCR probes used for qRT-PCR

Table S4. Antibodies used for immunoblots.

Supplementary Figures

Figure S1. *Dicer1* deletion in adipose tissue.

Figure S2. Lung angiosarcomas in *aP2-Cre;Dicer^{Flox/-}* mice.

Figure S3. Comparison of mouse and human angiosarcomas.

Figure S4. Interaction of miR~23~27~24 cluster with gene targets in angiosarcoma.

Supplementary Tables

Table S1. Enrichr analysis of upregulated genes ($p < 0.05$, log ratio of > 2.5) in angiosarcoma compared to normal aorta.

MicroRNA	P-value	Adj. P-value	Z-score	Comb. Score	Target Genes Enriched in Angiosarcoma
miR-23A, miR-23B	0.0004	0.0365	-1.88	6.21	<i>Adam19; Wsb1; Ccnd; Plau; Sema6d; Tfp2; Ammecr1; Rail4</i>
miR-520A, miR-525	0.0006	0.0365	-1.80	5.95	<i>Plxnd1; Ube2c; Sema6d; Pgf; Apln</i>
miR-191	0.0080	0.2618	-1.80	2.42	<i>Ammecr1; Sox4</i>
miR-324-3P	0.0093	0.2618	-1.77	2.37	<i>Adamts4; Wsb1; Plxnd1</i>
miR-338	0.0145	0.3278	-1.77	1.97	<i>Wsb1; Ccnd1; Sema6d</i>
miR-501	0.0188	0.3534	-1.67	1.73	<i>Ammecr1; Apold1; Sox4</i>
miR-491	0.0307	0.4343	-1.60	1.33	<i>Sema6d; B4galt5</i>
miR-224	0.0327	0.4343	-1.51	1.26	<i>Wsb1; Ammecr1; Kif23</i>
miR-34A, miR-34C, miR-449	0.0346	0.4343	-1.48	1.23	<i>Serpine1; Col12a1; Sema4c; Sox4</i>
miR-496	0.0427	0.4569	-1.52	1.19	<i>Sema6d; Emp1; B4galt5</i>
miR-202	0.0445	0.4569	-1.51	1.18	<i>Ccnd1; Rgs16; Nid2</i>
miR-27A, miR-27B	0.0561	0.5280	-1.64	1.05	<i>Adam19; Wsb1; Plxnd1; Plk2; Sema6d</i>
miR-138	0.0783	0.5473	-1.51	0.91	<i>Seema4c; Ammecr1; Sox4</i>
miR-107	0.0736	0.5473	-1.51	0.91	<i>Ammecr1; Kif23; Rail4</i>
miR-410	0.0645	0.5473	-1.39	0.84	<i>Rgs16; Rail4</i>
miR-506	0.0973	0.5549	-1.39	0.82	<i>Adam19; Wsb1; Sema6d; Ammecr1; Pgf; Apln</i>
miR-124A	0.0947	0.5549	-1.39	0.82	<i>Sema6d; Col12a1; Ccl2; Ammecr1; Rail4</i>
miR-24	0.0823	0.5473	-1.35	0.81	<i>Adam19; Mmp14; Ammecr1</i>
miR-15A, miR-16, miR-15B, miR-195, miR-424, miR-497	0.1233	0.5549	-1.31	0.77	<i>Sema6d; Col12a1; Ammecr1; Kif23; Apln</i>
miR-222, miR-221	0.1276	0.5549	-1.21	0.71	<i>Sema6d; Ammecr1</i>

Table S2. Antibodies used for immunohistochemistry.

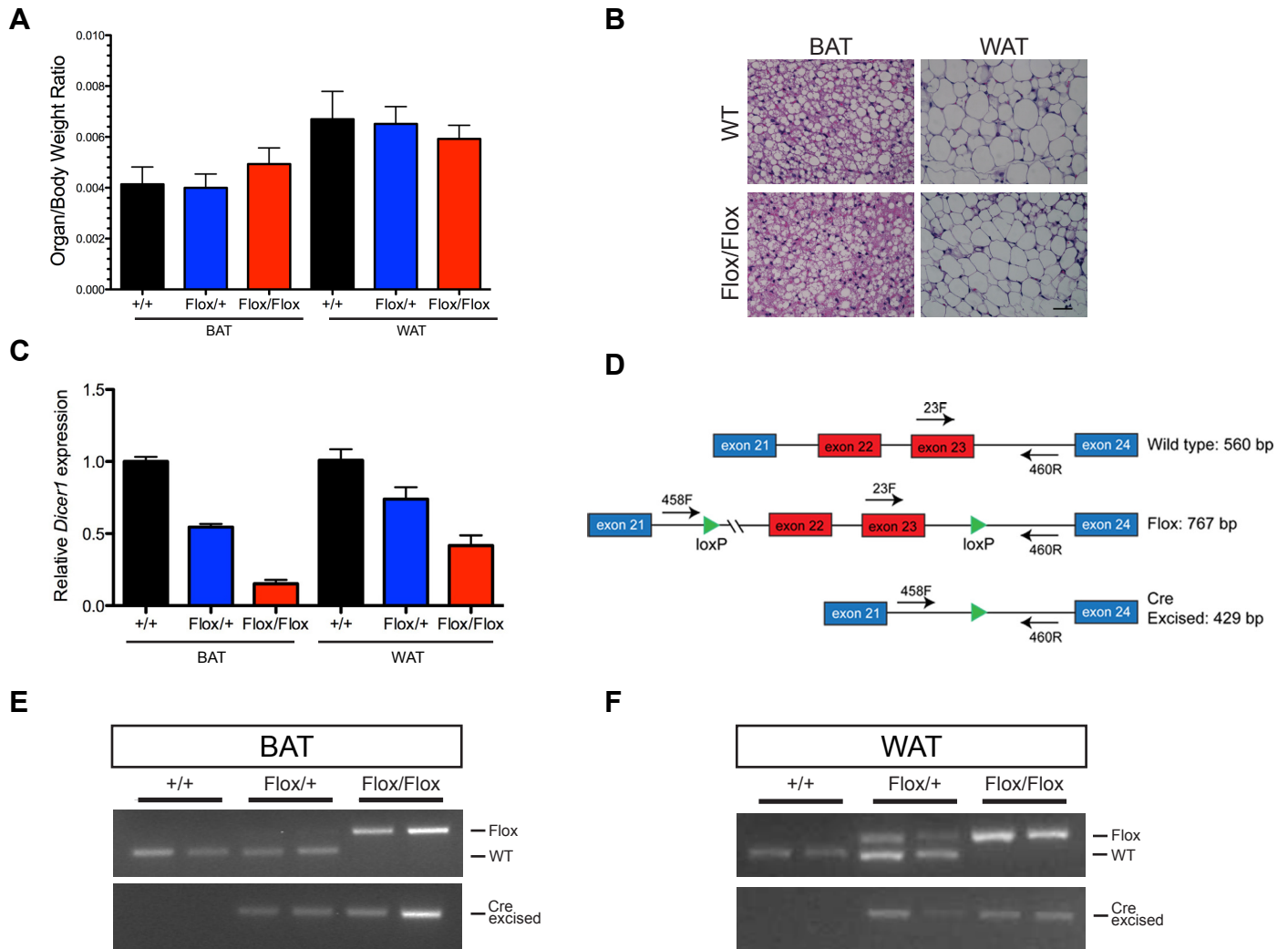
Antibody	Vendor	Catalog	Dilution	Retrieval	Retrieval Buffer	Detection
CD31	Histobiotec	DIA-310	1:100	HIER	CC1 (Roche)	Omap Rat (Roche)
CD34	BD Biosciences	553731	1:50	HIER	CC1 (Roche)	Omap Rat (Roche)
KI67	Thermo Fisher	RM-9106	1:100	HIER	CC1 (Roche)	OmniMap Rabbit (Roche)
MECA-32	BD Biosciences	553849	1:50	HIER	Target Retrieval pH 6 (DAKO)	Rat Polymer (Biocare Medical)
VEGFR2	R&D Systems	AF644	1:20	HIER	Target Retrieval pH 6 (DAKO)	Streptavidin-HRP (Thermo Fisher)

Table S3. Real-time SYBR primers and PCR probes used for qRT-PCR from Applied Biosystems.

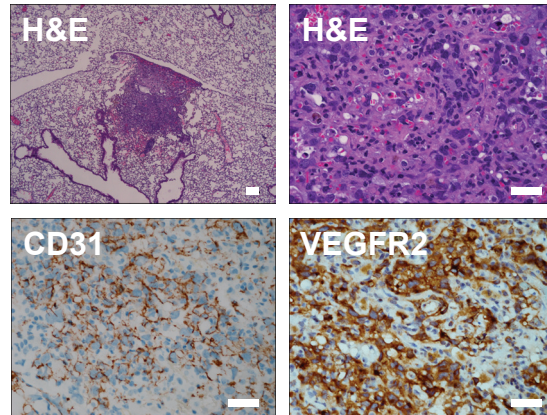
SYBR Primers		
Gene	Primer 1	Primer 2
<i>Adam19</i>	TTCTGTGTAGGCTGGAGCAA	GGAAAGCATCCACTCAGAGC
<i>Ammecr1</i>	TATGCATCCACGCAGTCTTT	CACCTGTACGGATACCAGCA
<i>Apln</i>	CTCGAAGTTCTGGGCTTCAC	CCTTGACTGCAGTTTGTGGA
<i>Aplnr</i>	ACTGGTTGTCAGCCCCATAG	CCCATCTCTGGAAGTGGTGT
<i>Ccnd1</i>	GGGTGGGTTGGAAATGAAC	TCCTCTCCAAAATGCCAGAG
<i>Plau</i>	ACAGATAAGCGGTCCTCCAG	GCCCCACTACTATGGCTCTG
<i>Rai14</i>	CCTTCTCAGCATCTCCGTTT	AGCCTGAAAGCAAAGTTTCG
<i>Sema6d</i>	GGCCAAGAAGAAATCTGAGC	CTTGTAGCCTGGAGCAGAGG
<i>Tfpi2</i>	GCAAGTCTGTTGGCAGAGGT	CAGAGACCAGCAAAGTGCC
<i>Wsb1</i>	GTCAAAGGAGCTGCTGGAG	CAGACGGTGCCCCATAGAT
Taqman Probes		
Gene	Assay ID	
<i>18S</i>	4308329	
<i>Dicer1</i>	Mm00521730_m1	
miR-23a-3p	000399	
miR-24-3p	000402	
miR-27a-3p	000408	
miR-126a-3p	002228	
miR-133b-3p	002247	
miR-182-5p	002334	
miR-183-5p	002269	
U6 snRNA	001973	

Table S4. Antibodies used for immunoblots.

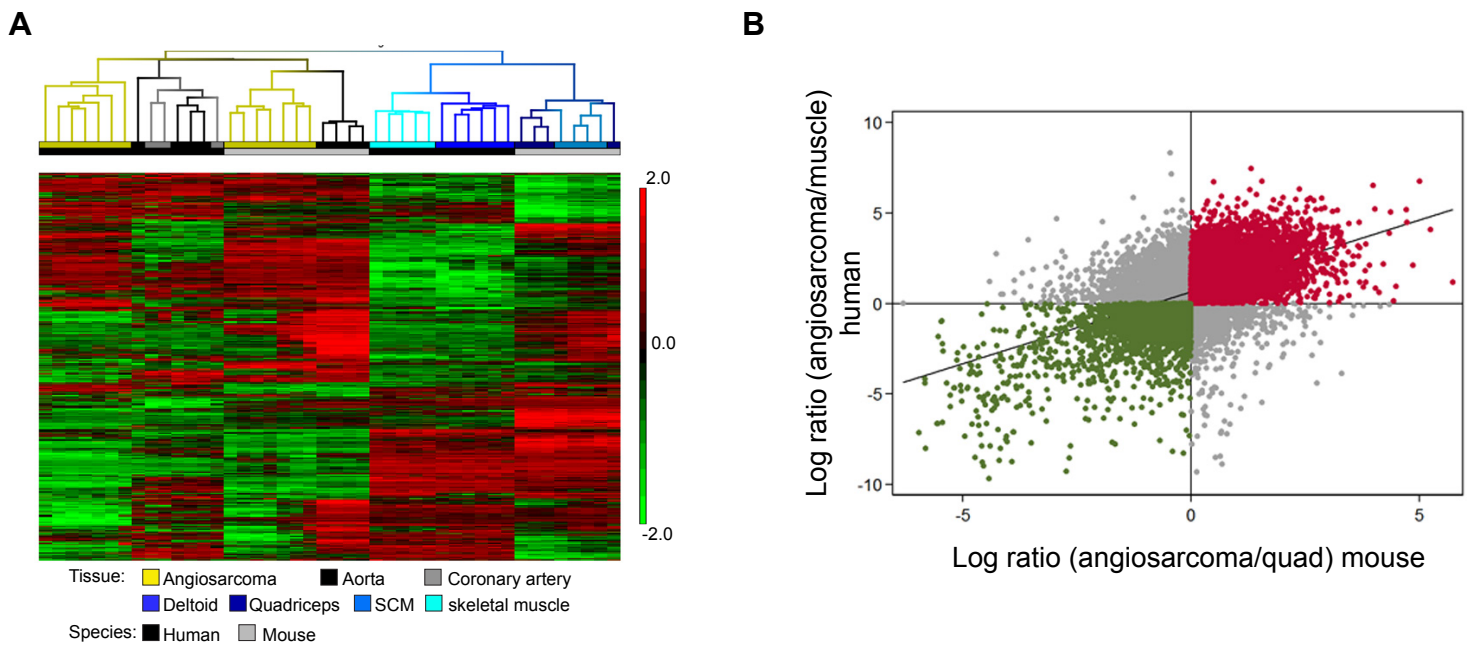
Antibody	Vendor	Catalog	Dilution
Phospho-p44/42 MAPK (ERK 1/2)	Cell Signaling Technology	9101	1:1000
p44/42 MAPK (ERK 1/2)	Cell Signaling Technology	9102	1:1000
Phospho-AKT (Ser473)	Cell Signaling Technology	4060	1:1000
AKT	Cell Signaling Technology	9272	1:1000
Phospho-S6 (Ser235/236)	Cell Signaling Technology	2211	1:1000
S6 Ribosomal Protein	Cell Signaling Technology	2217	1:1000
GAPDH	Millipore	MAB374	1:20000



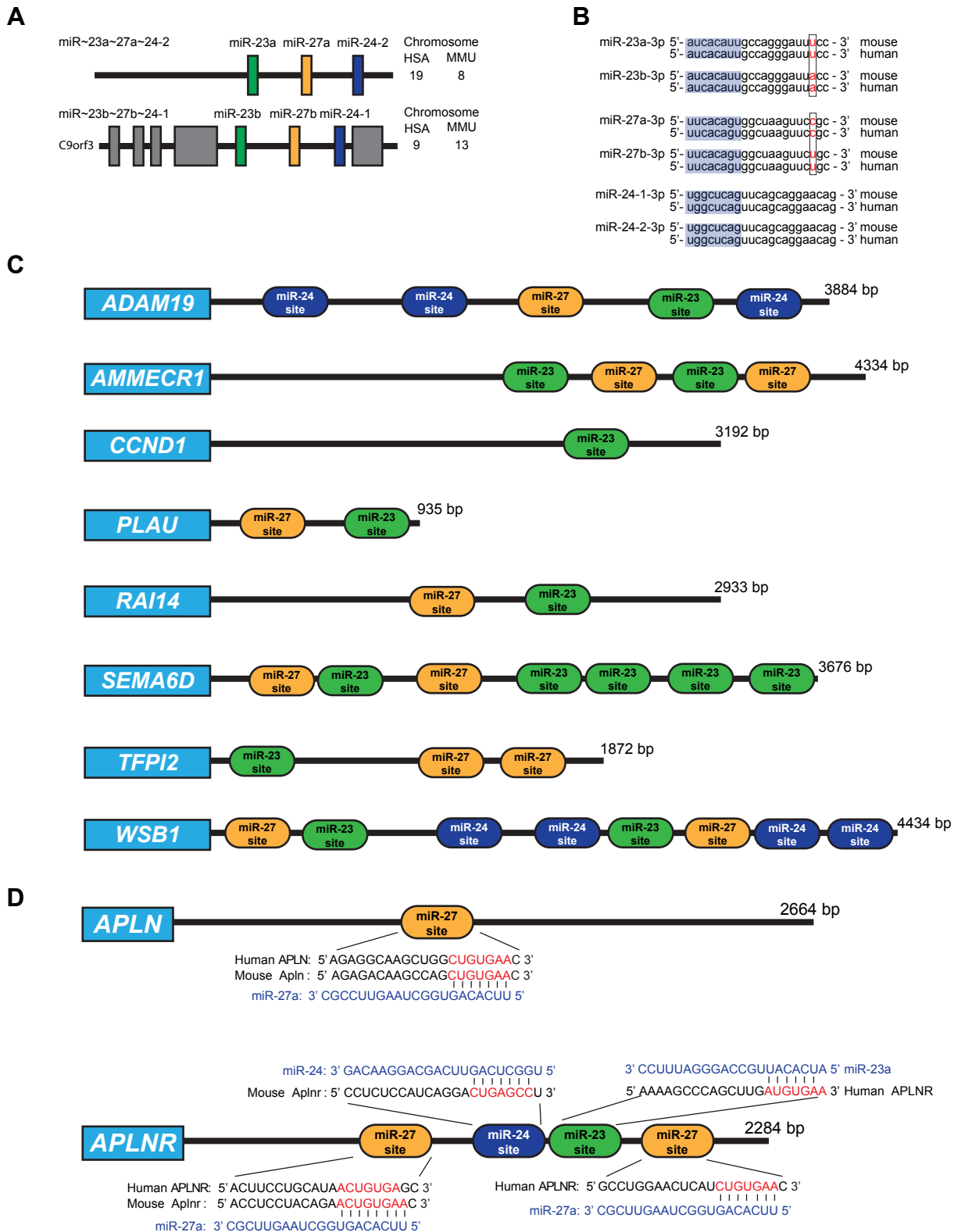
Supplementary Figure S1. *Dicer1* deletion in adipose tissue. (A) Interscapular brown adipose tissue (BAT) and inguinal white adipose tissue (WAT) weights relative to body weight in 24 day old $AD^{+/+}$, $AD^{Flox/+}$, and $AD^{Flox/Flox}$ mice ($n = 4$), and $P > 0.05$ for all comparisons. (B) BAT and WAT histology in $AD^{+/+}$ and $AD^{Flox/Flox}$ mice by H&E. Scale bar represents $25 \mu\text{m}$. (C) *Dicer1* expression by qRT-PCR in inguinal WAT and interscapular BAT from $AD^{+/+}$, $AD^{Flox/+}$, and $AD^{Flox/Flox}$ mice ($n = 3$), $P < 0.05$ for all BAT comparisons. $P < 0.05$ for all WAT comparisons except $AD^{+/+}$ compared to $AD^{Flox/+}$, $P = 0.0758$. (D) Schematic of *Dicer1* alleles and genotyping primers to detect the Wild type, Flox, and Cre-recombined alleles. Genomic PCR for *Dicer1*^{Flox} recombination in normal BAT (E) and WAT (F) from *AD* mice.



Supplementary Figure S2. Lung angiosarcomas in *aP2-Cre;Dicer^{Flox/-}* mice. H&E and IHC for CD31 and VEGFR2 from lung angiosarcoma in *AD^{Flox/-}* mice. Scale bar, 100 μ m in upper left image, otherwise 25 μ m.



Supplementary Figure S3. Comparison of mouse and human angiosarcomas. (A) Unsupervised hierarchical clustering analysis; Boxes below dendrogram signify tissue type (top row) and species (bottom row, human in black and mouse in gray). Tissues displayed: angiosarcomas (yellow), skeletal muscles (blue), coronary artery (gray) and aorta (black). Each column represents a distinct sample and each row a distinct gene. **(B)** Comparison of mouse angiosarcoma (n = 7) to human angiosarcoma (n = 7) with 13,267 orthologous genes plotted and 62% agreement in genes overexpressed (red) compared to muscle and underrepresented (green). Pearson's correlation coefficient = 0.49.



Supplementary Figure S4. Interaction of miR~23~27~24 cluster with gene targets in angiosarcoma. (A) Gene structure of miR~23a~27a~24-1 and miR~23b~27b~24-2 clusters showing chromosome locations in human and mouse. miR-23a/b, miR-27a/b and miR-24 are shown as colored boxes, the exons of the C9orf3 host gene of the miR-23b cluster are shown as gray boxes. **(B)** mature miRNA sequences of the miR~23~27~24 cluster miRNAs highlighting the seed sequences (blue boxes) and nucleotide differences between a and b miRNAs (red). **(C)** Schematic of miR~23~27~24 sites in genes enriched in angiosarcoma. **(D)** Schematic of miR~23~27~24 sites in the 3'UTR of APLNR and APLN.